Delineating Geothermal Structure from 3D Joint Inversion of MT and Gravity Data

W. Soyer[1], R. Mackie[1], S. Hallinan[1], F. Miorelli[1], A. Pavesi[1]

[1] CGG

Summary

We have implemented 3D faults as discontinuity surfaces, of finite extent, in the regularization step of our non-linear inversion engine (RLM-3D), for both single domain and cross-gradient joint inversion cases, and applied this for geothermal magnetotellurics (MT) and gravity inversion models: firstly for a synthetic graben case, and then on data from Sorik Marapi, a geothermal field located on the Great Sumatran Fault. Through integrated, quantitative modeling of multiple geophysical data types over geothermal fields, now including faults as sharp discontinuities, we facilitate geologically and structurally reliable multi-property 3D earth models that consistently explain the observations of available geophysical datasets.

Introduction - faults as regularization tear surfaces

At volcanic-hosted, high enthalpy, geothermal fields the subsurface resistivity reflects primary lithology, secondary (hydrothermal) alteration grade and intensity, temperature, porosity and pore fluid salinity (Ussher et al., 2000; Cumming, 2009). Broadband magnetotellurics (MT) surveys, responding to the 3D resistivity distribution from a few tens of meters down to tens of kilometers depth, are therefore the most commonly employed geophysical technique during geothermal resource exploration. Ground gravity commonly accompanies MT as it responds to *lateral* density contrasts such as significant fault systems, vertically-oriented intrusives, and/or propylitic-altered density anomalies.

Since the petrophysical relations between density and resistivity are far from straightforward in geothermal settings – varying across different lithology types – in joint inversion, we impose a structural similarity constraint between these properties using a 3D cross-gradient implementation. Following on from geothermal applications of cross-gradient joint inversion of MT, gravity and microearthquake data, described in Soyer et al (2018), we have now implemented fault surfaces as truly sharp discontinuities. The smoothness of regularization normally applied across the inversion cube can be interrupted with "tears" in the regularization process, defined along surfaces. To facilitate geologically-reasonable fault extents, we allow finite surface areas to be used, where the tear in the regularization also ends. A synthetic faulted system is illustrated firstly, followed by inversion of measured MT and gravity data from Sorik Marapi, a geothermal field on the Great Sumatran fault.

Synthetic faulted system

Using real topography borrowed from a similar setting, a conceptual geothermal system was built with an up-doming, resistive and dense reservoir zone below a conductive and lower density clay alteration cap (Figure 1). The main graben fault tears extend to 3km depth. The simulated geothermal field is *adjacent* to the graben structure, with typical three-layer scenario configured east of the graben and homogeneously resistive and denser "basement" rock to the west; the cross-section in Figure 2 (top row) illustrates the resistivity and density models.

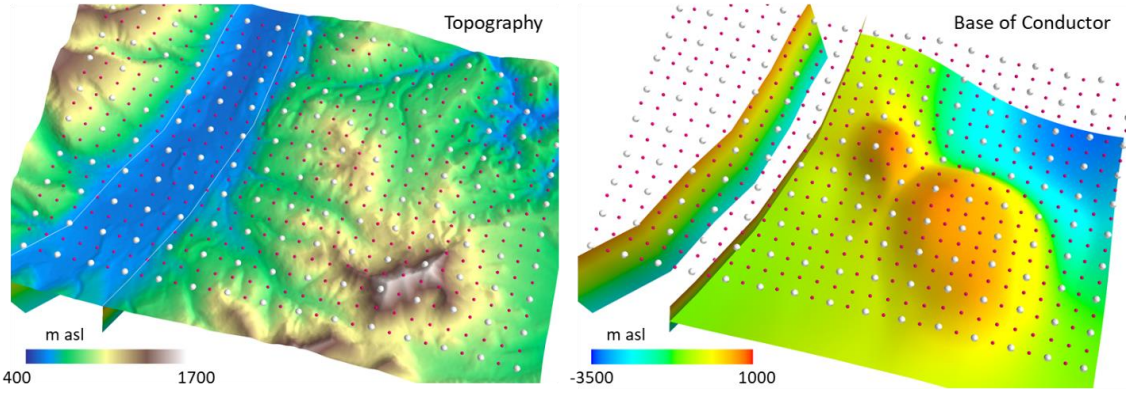

Figure 1 *Simulated structural setup of geothermal field, showing graben faults at surface (left) and projected below on the elevation of Base of Conductor (right). With MT (white) and gravity (red).*

All MT and gravity inversions started with homogeneous, half-space resistivity and density models. The single domain MT and gravity inversion models are shown in Figure 2 (left and right) with and without the use of regularization with tears at the faults (middle and bottom rows). While some detail at the base of conductor "cap" is missing, recovering the overall resistivity structure poses no major challenge to the MT inversion. As is the general case for unconstrained gravity inversions, however, while the lateral variations in density reflect the true case, the depth sensitivity is poor. Use of regularization with tears at the main faults results in sharper changes at the graben flanks – primarily to the west, and for gravity, which has a stronger integrated density change across the fault, also to the east. Structure recovery certainly improved *with* the tears.

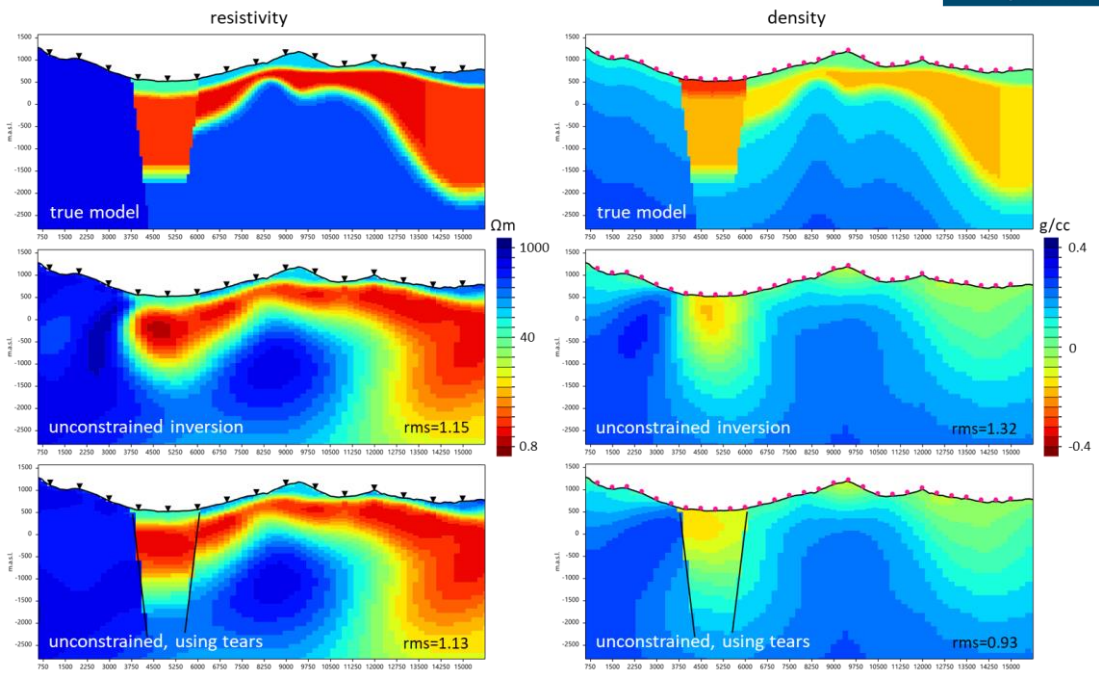

Figure 2 *Synthetic modeling of MT (left) and gravity (right): true model structure (top); unconstrained single domain inversions without (center) and with (bottom) faults as regularization tear surfaces. Density scale is variation from 2.40 g/cc. V.E. = 1.5.*

Cooperative (sequential) inversions and finally simultaneous joint inversions were then run. For the cooperative gravity inversions (Figure 3, left) the single domain *MT* inversion output (Figure 2 bottom left) was used as a fixed structural reference gradient model (cf Soyer et al 2018) during the *gravity* inversion. The simultaneous MT+gravity joint inversion (Figure 3 right) used a straightforward cross-gradient link between the MT and gravity inversion models, without a fixed reference model. The structure of the two density inversions (colour grids) is compared with the corresponding resistivity model (line contours, top row) and the true density model (line contours, bottom row). In the central model area, the density structure recovery in both inversions has improved significantly over the single domain result. In the graben the low-density zone is now modelled as a focused anomaly, as in the MT inversion model. However, as in all the gravity inversions here, the near-surface low density zone is not resolved (Figure 1 top right).

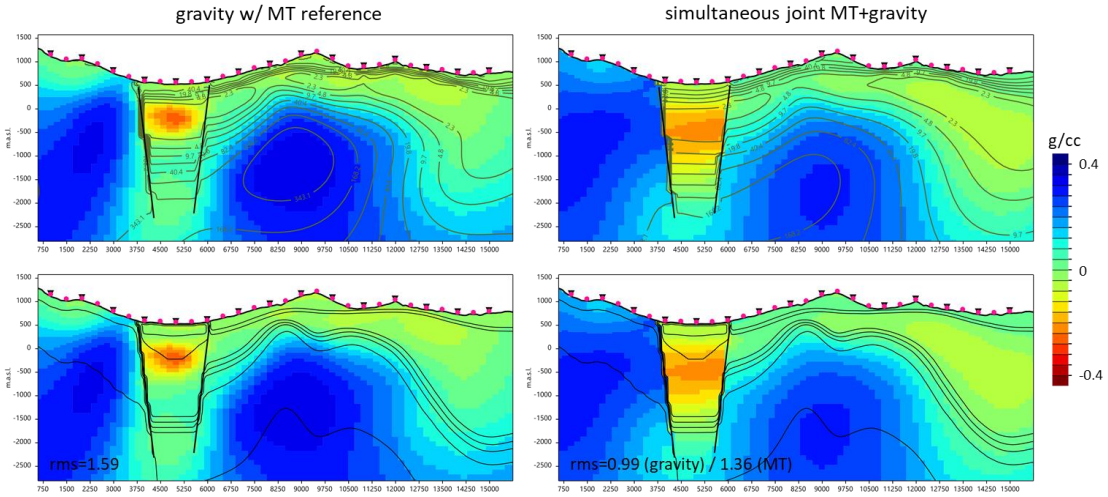

Figure 3 *Cross-gradient gravity inversions including fault tears (all colour grids = density). Left: using the single domain MT inversion result as a structural reference. Right: simultaneous joint gravity+MT inversion. Top and Bottom compare the density inversions with line contours from the corresponding resistivity model (top) and the true density model (bottom). VE=1.5.*

Sumatra fault system – Sorik Marapi

The Sorik Marapi geothermal field (Sagala et al., 2016) is located *within* the low density, volcano-sedimentary sequence of the pull-apart graben structures along the main Sumatra fault, flanked by outcropping high density pre-Tertiary metamorphics (Figure 4). The Bouguer gravity reflects the graben structure, particularly the flanks where the strongest gravity gradients are observed (Figure 4). The fault delineations used in the inversion modeling are taken from geological maps where the faults outcrop, and from the gravity gradient maxima where not. Steep, normal fault dips of 80° were assumed, extending to 3km depth. These finite length tears in the regularization were tested in a suite of inversion runs (Figure 5). Bouguer gravity data were assigned a 0.3mGal error, and relative density changes were inverted with respect to the reduction density 2.40g/cc. MT data were inverted within the frequency band of 0.0016-2500Hz, with five frequencies per decade. All resistivity and density inversion starting models were homogeneous half-spaces.

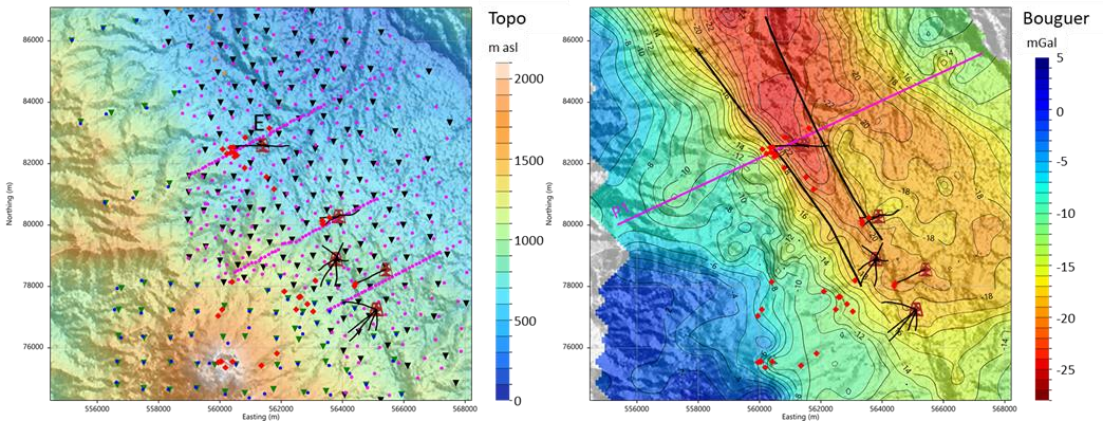

Figure 4 *Left: Sorik Marapi topography, showing SM volcano near southern margin, with MT (triangles), gravity (points), hot springs and fumaroles (red) and well traces. Right: Complete Bouguer gravity anomaly at 2.40g/cc, with reverse color scale (as resistivity). The two black NW-SE lines mark faults from surface geological mapping and tracing the gravity gradient maxima.*

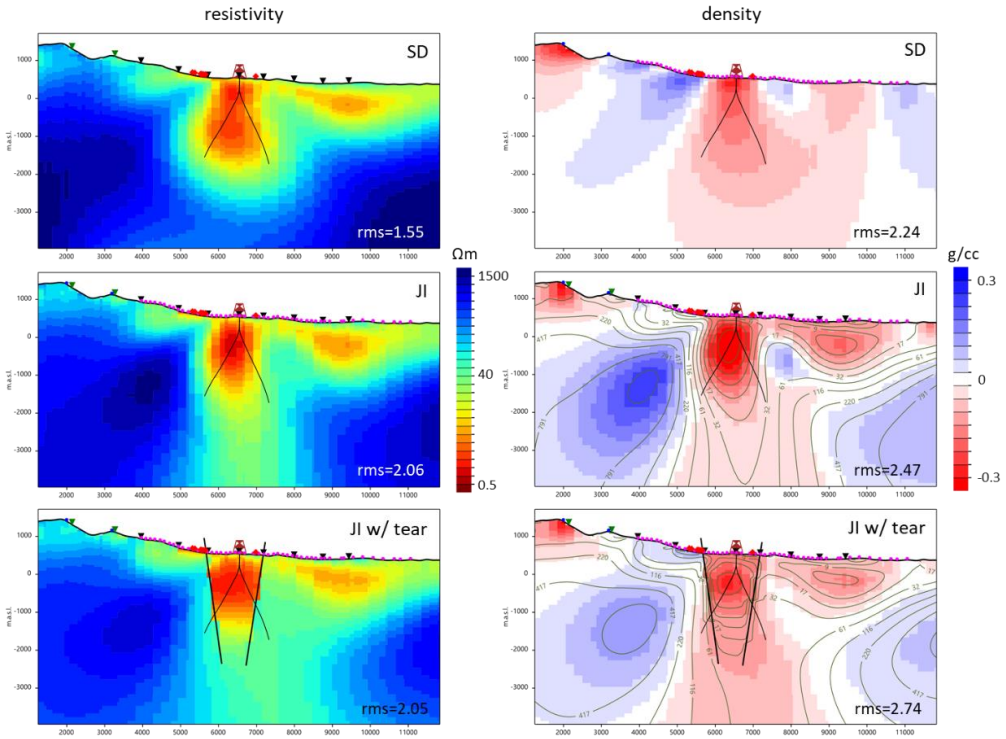

Figure 5 *Dip section through pad E well traces of MT (left) and gravity (right) inversions; single inversions (top) with cross-gradient joint inversions center (no faults) and bottom (with faults). VE=1.*

As in the synthetic example, and typical for MT and gravity data types, the MT inversions are more robust than the gravity ones, with little difference between single and joint domain outputs within the depths of interest, while gravity inversions improved considerably with the inclusion of shallow depth information from the MT models. The use of regularization with tears at the faults results in sharp boundaries specifically at the western limit of the graben, and accordingly less artifacts (lower overshoot to higher resistivity) from the smoothing. The fault intersections along the two pad E wells were unknown during the inversion modeling exercise. Methylene blue data (MeB, sensitive to smectite) from one well became available *after* the inversions. These are overlain on the joint gravity+MT inversion with tears (Figure 6), showing excellent MeB correlation with the resistivity break at the modeled fault location.

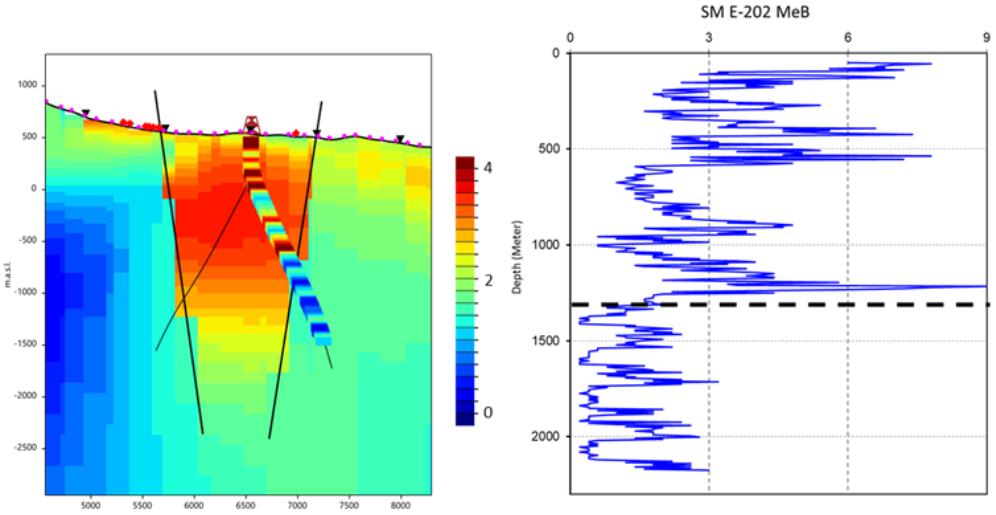

Figure 6 *Left: resistivity from joint gravity-MT inversion + fault tears (grid colour scale as Figure 5) with MeB summary overlain along the well trace. The MeB color bar (center) refers to the smoothed MeB readings. Right: MeB log with modeled fault location projected at the black dash.*

Conclusions

We have implemented 3D faults as discontinuity surfaces, of finite extent, in the RLM-3D inversion regularization, and used the scheme during both single domain and cross-gradient joint inversions of geothermal MT and gravity datasets, firstly for a synthetic case, and then for the Sorik Marapi field data. Through integrated, quantitative modeling of multiple geophysical data types over geothermal fields, now including faults as sharp discontinuities, we facilitate geologically and structurally reliable multi-property 3D earth models that consistently explain the observations of different geophysical datasets.

Acknowledgements

Thanks to KS Orka Renewables (Indonesia) for permission to include the Sorik Merapi results.

References

Cumming, W. [2009]. Geothermal Resource Conceptual Models Using Surface Exploration Data, *Proceedings, 34th Workshop on Geothermal Reservoir Engineering, Stanford University*.

Sagala, B.D., Chandra, V.R., and Purba, D.P. [2016]. Conceptual Model of Sorik Marapi Geothermal System based on 3-G Data Interpretation, *ITB International Geothermal Workshop, Bandung*.

Soyer, W., Mackie, R.L., Hallinan, S., Pavesi, A., Nordquist, G., Suminar, A., Intani, R. and Nelson, C. [2018]: Geologically-consistent Multiphysics Imaging of the Darajat Geothermal Steam Field, *First Break, 36 (6) 77-83.*

Ussher, G., Harvey, C., Johnstone, R., and Anderson, E. [2000]. Understanding the Resistivities Observed in Geothermal Systems. *Proceedings, World Geothermal Congress, Kyushu-Tohoku*.